Mechanical Testing and Diagnosis
ISSN 2247 – 9635, 2014 (IV), Volume 4, pp. 5-16

# NEW MATHEMATICAL MODEL FOR POINT CONTACT TRANSITION FROM ELASTIC TO ELASTO-PLASTIC FIELD. EXTENSION FROM NORMAL CONTACT ELLIPSE TO CUTTING POINT CONTACT

**Daniel REZMIRES**

S.C. SIRCA S.A – Piatra Neamt, Romania
drezmir@hotmail.com

**ABSTRACT**

*This document offers a new numerical solution to analyze the transition from Hertzian point contact in elastic field to elasto-plastic and full plastic contact as function of Brinell Hardeness number, considering uniform Yield in subsurface. The method takes into account a slice techniques and surface HB value limitations. Results are compared to literature data for Hertz point contact and with standard test method for Brinell hardness.*

**Keywords:** Hertz contact, non-Hertz contact, elasto-plastic, Brinell Hardeness number (nHB), cutting point contact, contact ellipse

## 1. INTRODUCTION

Literature presents relations between normal contact pressure and subsurface stress for elastic contact [1, 2, 3]. The elastic-plastic contact of a sphere and a flat body is a fundamental problem in contact mechanics. In this model, the Brinell hardeness sphere is higher like the raceway hardness and the stresses remain in the elastic Hertzian contact domain. Literature presents different studies to approximate the transition between elastic to plastic contact, as for example, references [7, 8, 9]. Reference [6] presents the Brinell test method and the imprint parameters under the effect of external load as a function of HB number (nHB). The analysis is made using a slice technique method presented in [4, 5].

## 2. NUMERICAL FORMULATIONS OF THE LINEAR DEPENDENCE BETWEEN LOAD AND THE SLICE CONTACT DEFORMATION IN ELASTIC FIELD AND ELASTO-PLASTIC

According to Hertz theory, the link between the maximum central contact pressure P0 in a point contact and the shear stress $\tau$ in subsurface is given as $\tau = 0.3 \cdot P0$. If Pm is the mean contact pressure in a slice, then $P0 = 1.5 \cdot Pm$. Usually, the yield limit as a function of Brinell hardness is approximate as $\sigma 02 = 2.7 \cdot nHB$, where nHB is the Brinell Hardness number [6]. With these assumptions, it results:

when $\tau=\sigma02/2 \Rightarrow P0\tau=6.75\cdot nHB$ and $Pm\tau=4.5\cdot nHB$ (1)
when $\tau=\sigma02 \Rightarrow P0\tau=13.5\cdot nHB$ and $Pm\tau=9.0\cdot nHB$

In the equation (1), $Pm\tau$ represents the mean contact pressure, which produces the shear stress $\tau$, $P0\tau$ is the maximum contact pressure, which produces the shear stress $\tau$.

According to [4, 5], a slice "j", from a contact, displaced with ($\xi$) from a real contact, can be described with following parameters:

Local contact pressure, P=P(j)
$$P_j \approx \frac{0.282\cdot E0\cdot k_j^{-0.11}\cdot\delta_j\cdot 2}{\pi\cdot b_j} fp(k_j), \text{ with} \quad (2a)$$
$$fp(k_j)=\frac{3.2821-0.3322\cdot\ln(k_j)}{1+0.42877\cdot\ln(k_j)}$$

Local semi-width, b=b(j)
$$b_j = R_{y_j}\cdot\sqrt{\frac{\delta_j\cdot k_j^{-0.11}}{Ry}}1.15617\cdot fb(k_j), \text{ with} \quad (2b)$$
$$fb(k_j)=\frac{1.21386-0.07678\cdot\ln(k_j)}{1+0.115078\cdot\ln(k_j)}$$

Local load,
$$Q_j = E0\cdot k_j^{-0.11}\cdot\delta_j\cdot\Delta x_j\cdot fQ(k_j) \text{ with} \quad (2c)$$
$$fQ(k_j)=\frac{0.94896-0.09445\cdot\ln(k_j)}{1+0.45412\cdot\ln(k_j)}$$

In equations (2a)...(2c), the following notations are done: E0 is eqivalent modululs of elasticity of the two bodies in contact, it can be $E_j$ (if local inclusions exists in the slice j), $k_j$ is the local elipticity in the slice; $fQ(k_j)$, $fb(k_j)$, and $fp(k_j)$ are interpolation functions used to create a linear dependence of contact relative approach, $\Delta x_j$ is the length of the slice section *"j"*, $\delta_j$ is the local approach corresponding to slice j, $Q_j$ is load on slice j.

Two non-dimensional paramaters were computed using equation (1), as follows:
fPPm=[(13.5+9)/2]/13.5=0.833 (3)
mPPm=0.5(2/3+fPPm)·[1….1.03]≈ 0.77 (for metalic material)

According to equations 1, 2 [4, 5] and 3, when the elasto-plastic field materializes, then (2a) and (2c) formulas become:

$$Q(j)\approx 2\cdot b(j)\, P0\,\tau\, \Delta x_j\cdot mPPm\cdot f(HB), \text{ with } f(HB)\approx 0.96 \quad (4)$$
$$\text{and } P(j)= P0\,\tau$$

## 3. NUMERICAL VALIDATION OF THE PROPOSED MODEL IN THE CIRCULAR POINT CONTACT CASE

Equations 2, 3 and 4 are applied in a slice technique method presented in [5]. According to [6], a 10.00 mm ball is considered. The contact conformity is modified in simulation and a constant load of 3000 kgf is applied. Some different values for nHB are considered to show the transition between Hertzian contact and plastic field in Brinell test. Six different cases were considered as follows:

***Case 1. 100 HB*** [6]

If the material is characterized by a hardness of 100 HB, the contact parameters are shown in Fig. 1. Figure 1a presents the contact pressure computed with Hertz theory [4, 5] and the relations without taking into account the material hardness (nHB) and also the proposed model with a HB limit. Figure 1b presents the shape (circle or ellipse) computed with Hertz relations, equation (2) from [4, 5], without taking into account the material hardness (nHB) and also the shape resulted with the model considering the HB limit of the material. Figure 1c presents the shape of local loads in slices, computed with Hertz relations, equation (2) from [4, 5], without taking into account the material hardness (HB) and also the load diagram in slices, as resulted from the HB limit of the material. Figure 1d presents the shape of indentation in slices as computed from the model proposed to consider the material hardness HB.

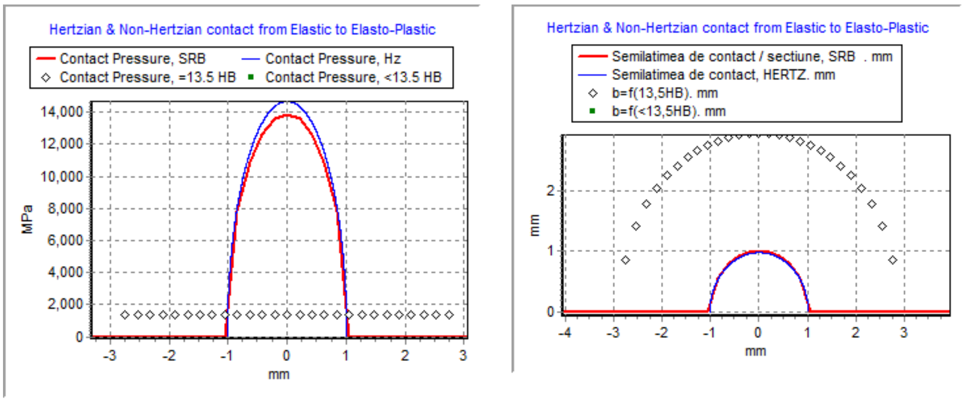


a) Contact pressure b) Contact shape

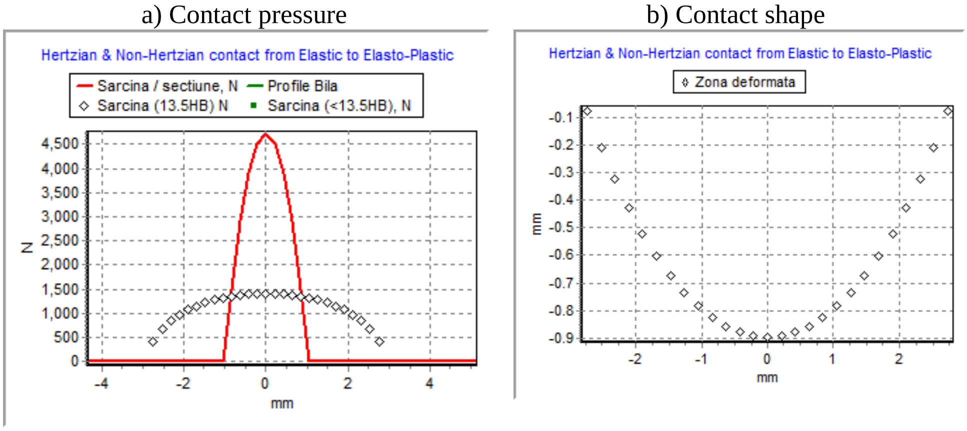


c) Load in the contact slice d) Indentation shape

Fig. 1.

According to [6], Figures 1b and 1d point out that the results have an excellent correlation.

***Case 2. 400 HB [6]***

If the material has a hardness of 400 HB, the contact parameters are shown in Fig. 2.1. Fig. 2.1a presents the contact pressure computed with Hertz theory and [4, 5] relations, without to take into account the material HB and also the proposed model with HB limit. Fig. 2.1b presents the contact shape (circle or ellipse) computed with Hertz relations and equation (2) from [4, 5], without taking into account the material HB and also the shape resulted with actual model, considering the HB limit of the material. Fig. 2.1c presents the shape of loads in slices computed with Hertz relations, equation (2) from [4, 5], without taking into account the material hardness HB and also the load diagram in slices, resulted with the HB limit of the material. Fig. 2.1d presents the shape of indentation in slices computed with the actual model taking into account the material hardness HB.

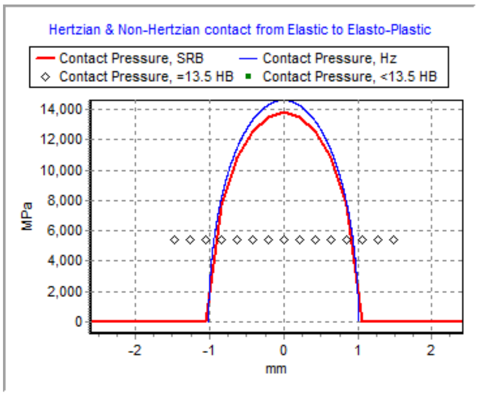


a) Contact pressure

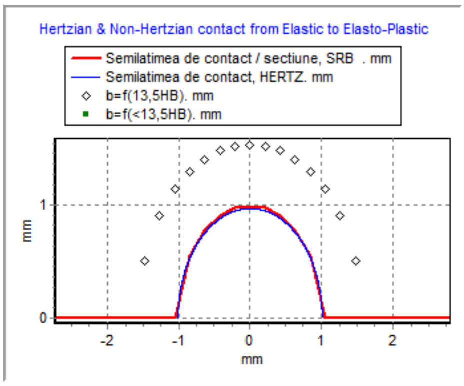


b) Contact shape

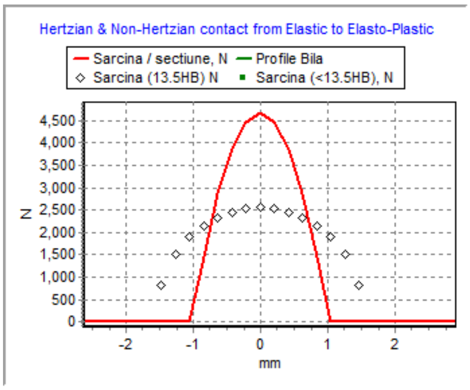


c) Load in the contact slice

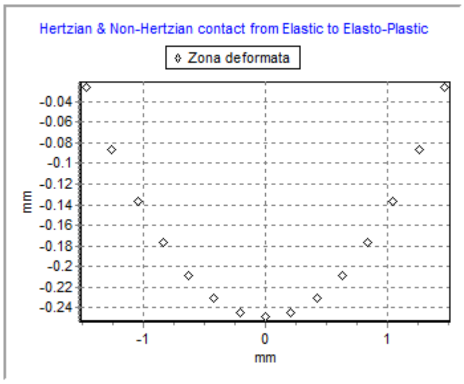


d) Imprint shape

Fig. 2.1.

According to [6], the results are in an excellent correlation in Fig 2.1b and Fig 2.1d.

If the process is repeated for all HB numbers, then the resulted form [6] will be retrieved.

If material has a hardness of 400 HB, two different loads are applied to show the algorithm evolutions according to Figure 2.2 (a, b, c, d, e, and f). The load evolution contact parameter for 2 different normal loads. Fig 2.2 (a, b, c) corresponds to a normal load with 1682 N, when the first point with 13.5 HB local contact pressure appears. Figure 2.2 (d, e, f) corresponds to a normal load with 20693 N, when many points corresponds to limited contact pressure of 13.5 HB ($P0\tau = 13.5 \cdot nHB$).

A comparison between Fig 2.2a and Fig 2.2d, Fig 2.2b and Fig 2.2e and Fig 2.2c and Fig 2.2f shows the evolution contact parameters as a function of the external load value, when the HB number is considered.

1682 N, first point with 13.5 HB

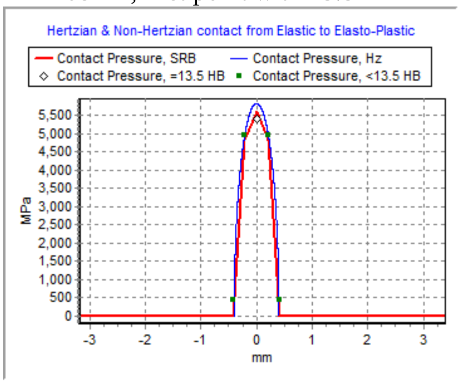


20693 N

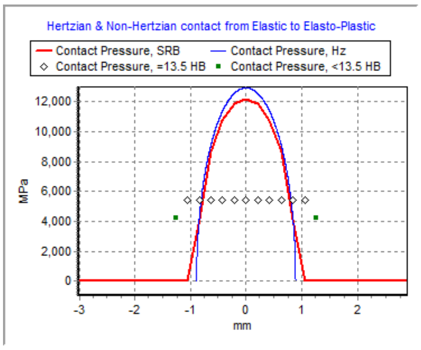


a) Contact pressure distribution

d) Contact pressure distribution

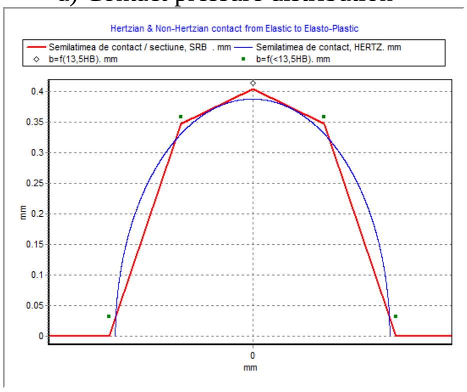


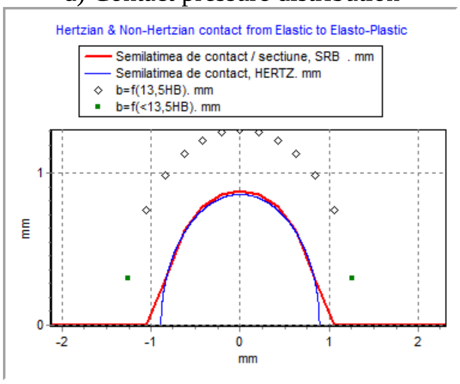


b) Contact zone shape (ellipse or circle)

e) Contact zone shape (ellipse or circle)

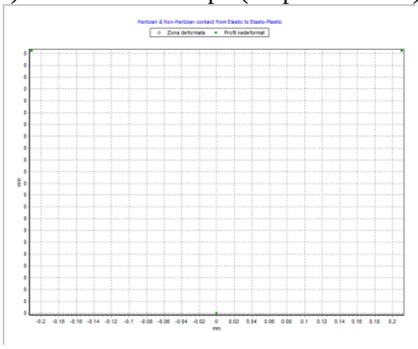

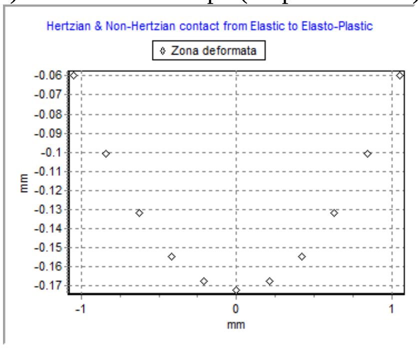


c) No indentation (elastic field)

f) Indentation (elastic-plastic field)

Fig. 2.2.

***Case 3. Continuous transition for 300 HB, example with 0.507 conformity, ball diameter of 20 mm***

If we consider a hardness of 300 HB and the specific contact geometry according to Fig. 3.1a, then the contact rigidity will result according to Fig. 3.1b. Figure 3.1b shows the 2 regions which correspond to loads with contact pressure less than 13.5 HB and point with elastic-plastic deformations.

If two different loads are applied, as for example, 51594 N and 74810 N, the contact parameters evolutions are according to Fig. 3.2 (a…f). Figures 3.2a, b and c correspond to a load of 51594 N, when the first point with 13.5 HB is revealed. Figures 3.2d, e and f correspond to a load of 74810 N, when many points with 13.5 HB exist, with elastic and elastic-plastic specifications.

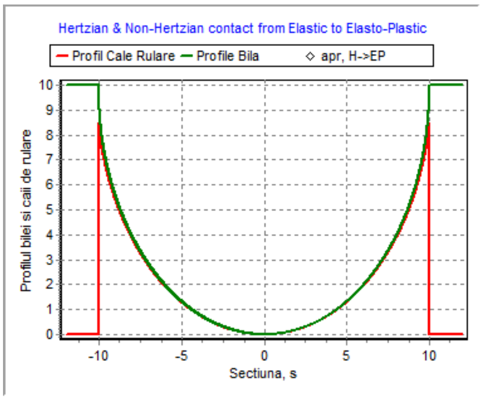


a) The contact geometry

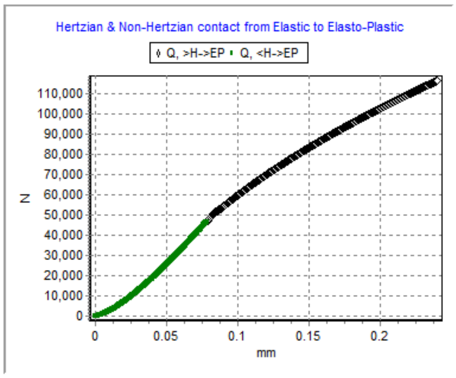


b) The contact rigidity

Fig. 3.1.

51594 N, first point with 13.5 HB

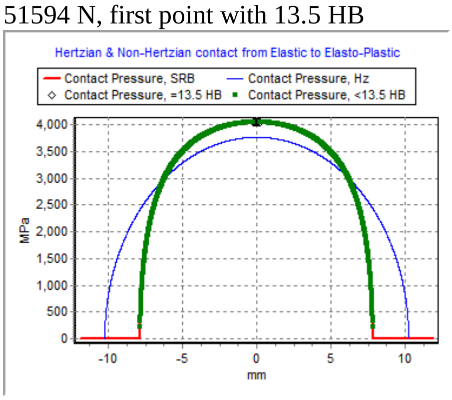


a) Contact pressure

74810 N

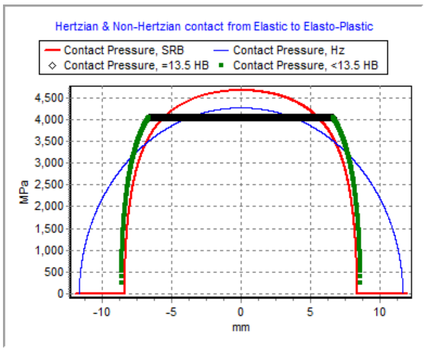


d) Contact pressure

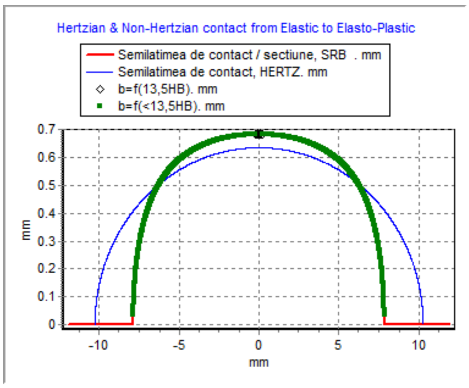


b)Contact area

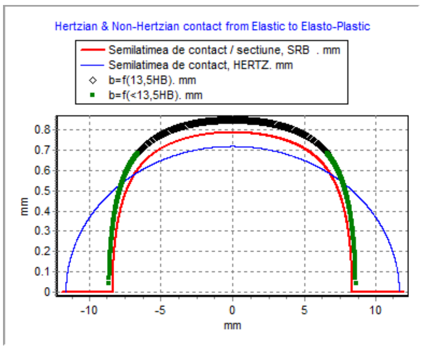


e) Contact area

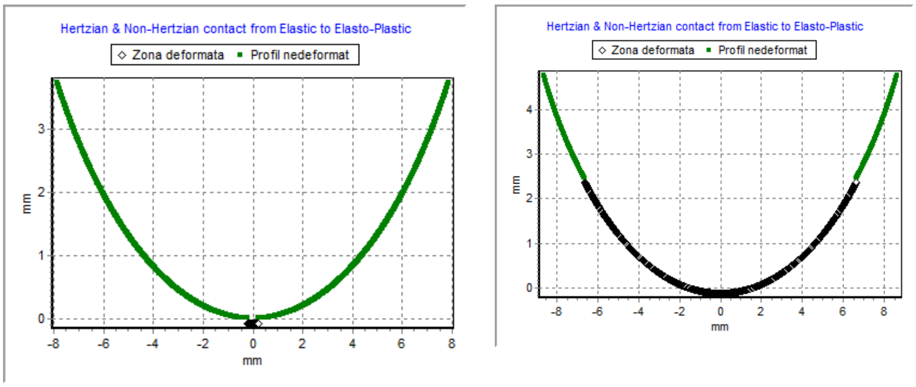


c) Final form of the raceway after load f) Final form of the raceway after load

Fig. 3.2.

***Case 4. Continuous transition for 300 HB example for 0.507 conformity, Ball diameter 20 mm, rs=2 mm, rd=2 mm, U=44***

Figure 4.1a and b corresponds to the contact geometry: Figure 4.1a presents the initial geometry and Fig 4.1b presents the contact region rotated with 44 degrees, which corresponds to the contact between a ball and a raceway, at 44 degrees. The two parameters, rs and rd, are the rayon radius and are 2 mm each, in this example.

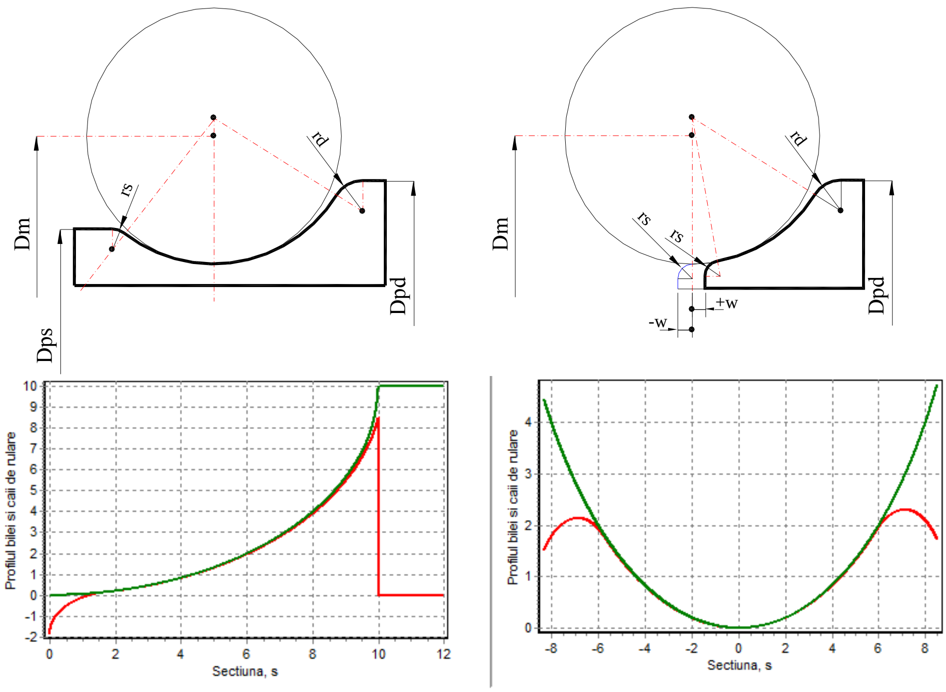


a) Initial contact geometry b) Rotated contact region

Fig. 4.1

To show the contact parameter evolution, two normal loads between a ball and a raceway are applied. Figure 4.2a, b, c and d corresponds to a normal load of 11649 N, when all points are less of 13.5 HB, and no truncation area contact exists.

Figure 4.3a, b, c and d corresponds to a normal load of 24618 N, when all points are less of 13.5 HB, and truncation area contact exists.

**11694 N**

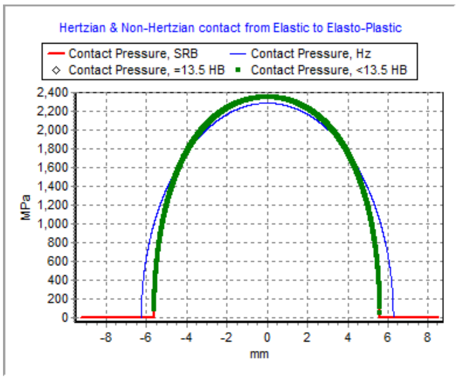


a) Contact pressure

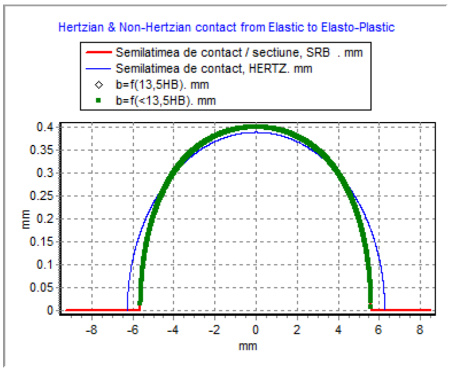


b) Contact ellipse


c) Shape of the load repartition

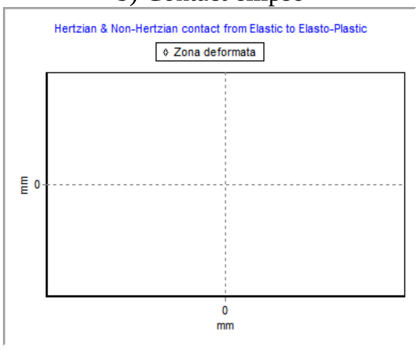


d) 0 imprint (elastic field)

Fig. 4.2.

**24618 N**

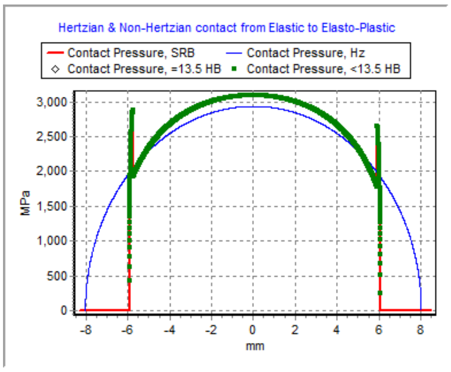


a) Contact pressure

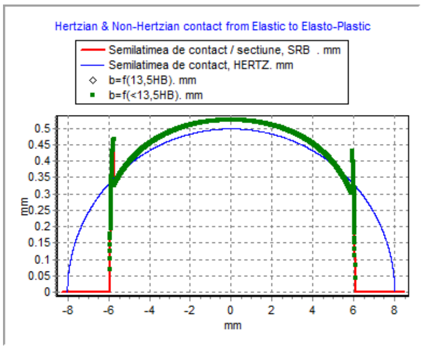


b) Contact ellipse

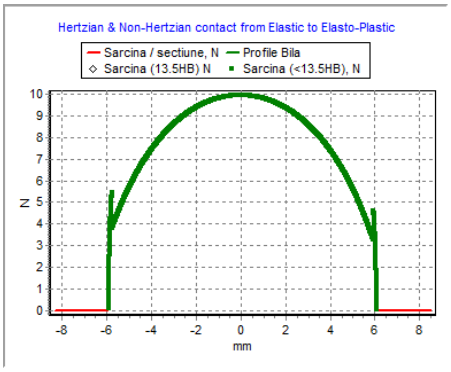


c) Shape of the load repartition

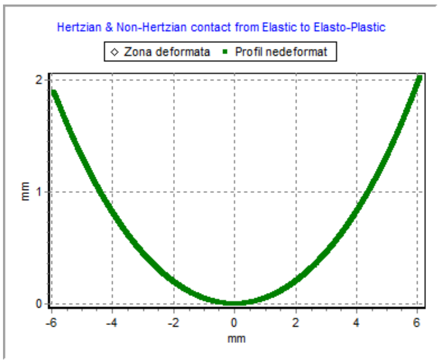


d) 0 imprint (elastic field)

Fig. 4.3

Figure 4.4 (a, b, c and d) corresponds to a load of 43276 N and 53383 N, respectively, when points with 13.5 HB exist and a truncation area contact exists, also.

Figures 4.4a and 4.4b show the contact pressure evolution while Figures 4.4c and d show the incipient indentation, in two regions, for 43276 N) and (3 regions with indentation under a load of 55383 N, respectively.

If another contact angle exists, as for example, 53 degrees, then the contact parameters will be different, as shown in Case 5.

| 43276 N – first points with 13.5 HB | 53383 N –more points with 13.5 HB |
|---|---|

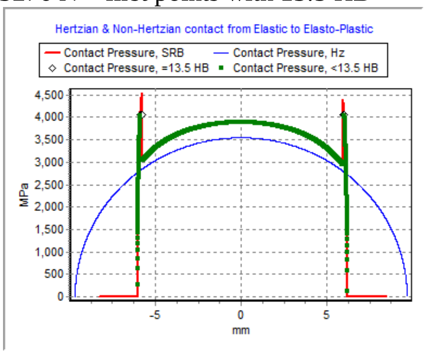


a) Contact pressure

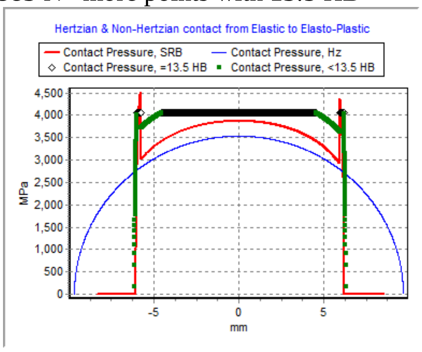


b) Contact pressure

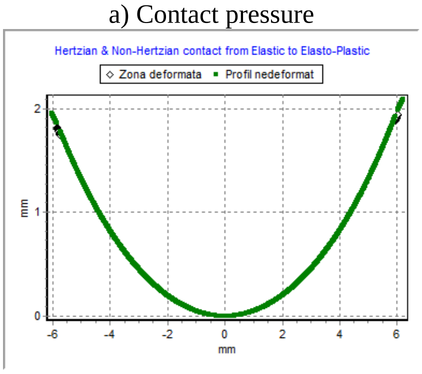


c) Small Indentation areas

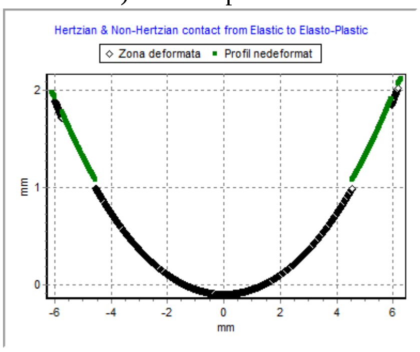


d) Large indentation areas

Fig. 4.4.

### *Case 5. Continuous transition for 300 HB example for 0.507 conformity, ball diameter of 20 mm, rs=2 mm, rd=2 mm, U=53*

Figure 5.1 a and b corresponds to a contact geometry. Fig. 5.1a presents the initial geometry and Fig 5.1b presents the contact region rotated with 53 degrees, which corresponds to the contact between a ball and a raceway at 53 degrees. The two parameters, rs and rd, are the rayon radius and are 2 mm each, in this example.

Proceeding in the same manner if a normal load is applied and the contact parameters are shown in Fig. 5.2a, b, c and d. In this case, the external load is 45128 N.

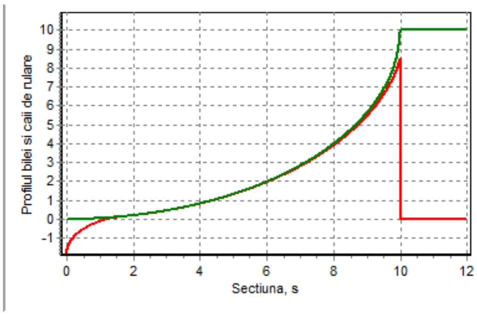


a) Initial contact geometry

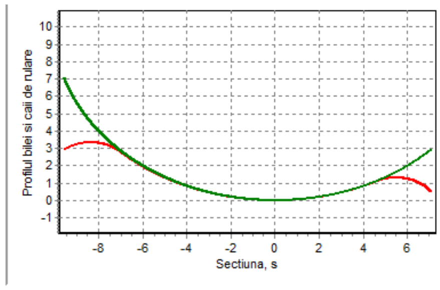


b) Rotated contact region

Fig. 5.1

**Q= 45128 N**

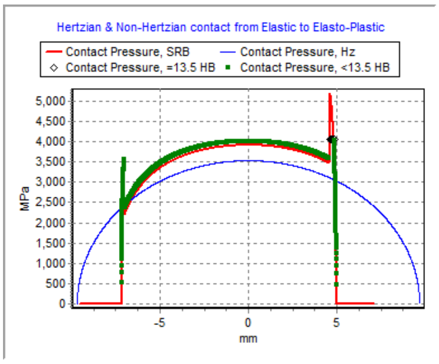


a) Contact pressure

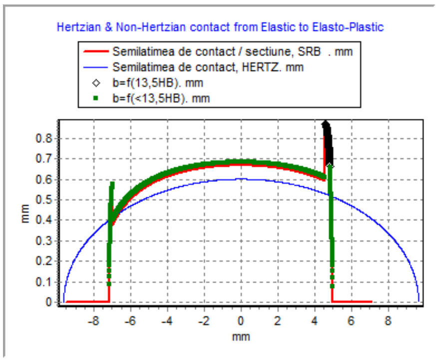


b) Contact area

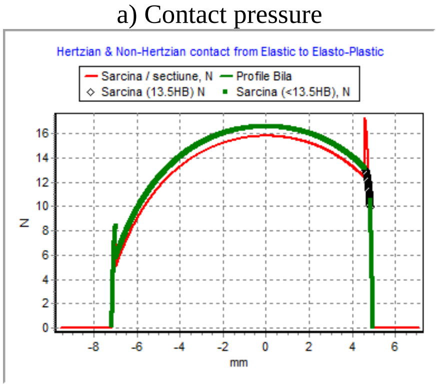


c) Load on slices

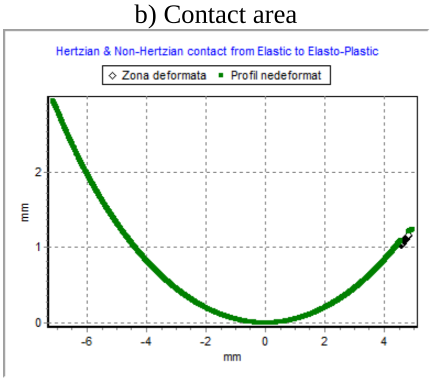


d) Small indentation region

Fig. 5.2.

***Case 6. Continuous transition for 300 HB, example for 0.507 conformity, ball diameter of 20 mm, rs=2 mm, rd=2 mm, U=18***

Figure 6.1a and b corresponds to a contact geometry. Figure 6.1a presents the initial geometry and Fig 6.1b presents the contact region rotated with 18 degrees, which corresponds to the contact between a ball and a raceway at 18 degrees. The two parameters rs and rd are the rayon radius and are 2 mm each in this example.

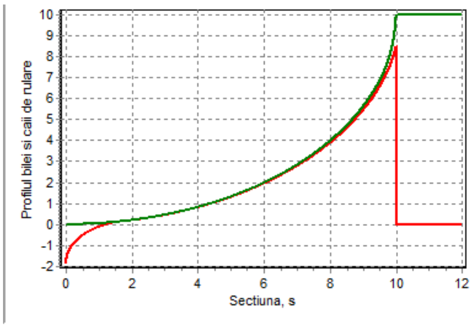


a) Initial contact geometry

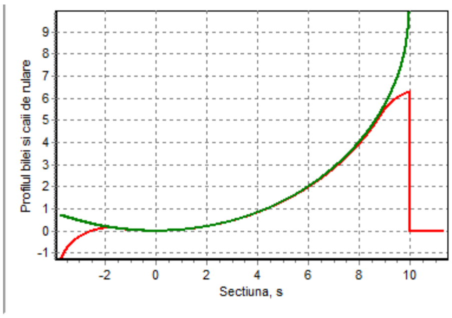


b) Rotated contact region

Fig. 6.1.

When a load of 23756 N is applied, then the contact parameters are shown in Fig. 6.2a, b, c and d. In this case, a small indentation area will appear.

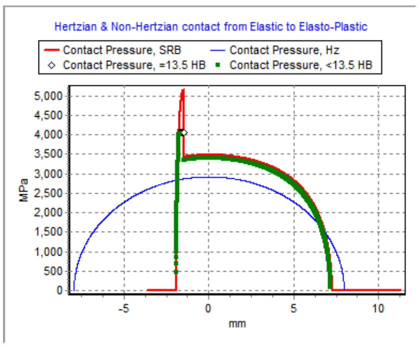


a) Contact pressure

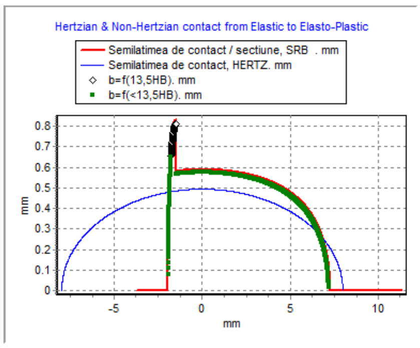


b) Contact ellipse parameter

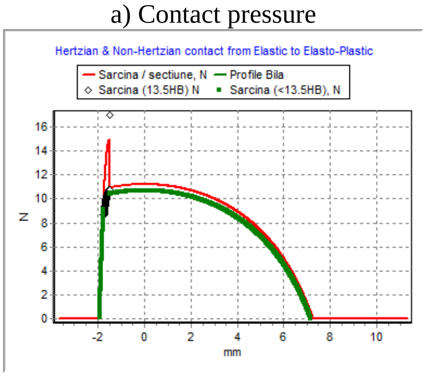


c) Load on slices

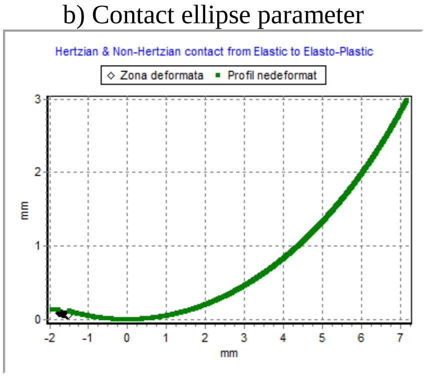


d) Small indentation area

Fig. 6.2.

When a load of 52377 N is applied, more points with 13.5 HB will appear and the contact parameters are shown in Fig. 6.3a, b, c and d, as follows.

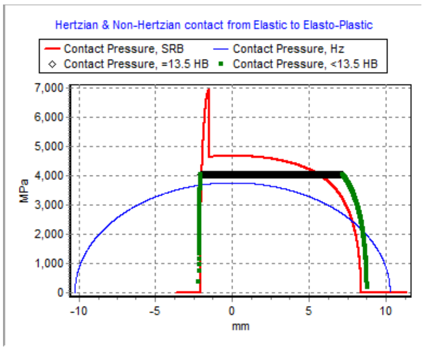


a) – Contact pressure

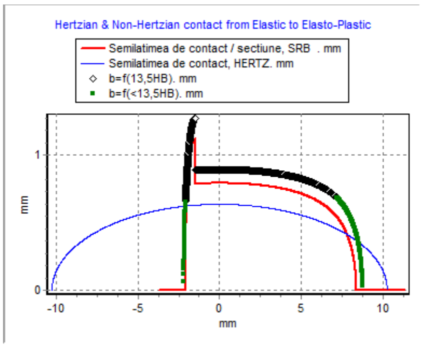


b) – Contact ellipse

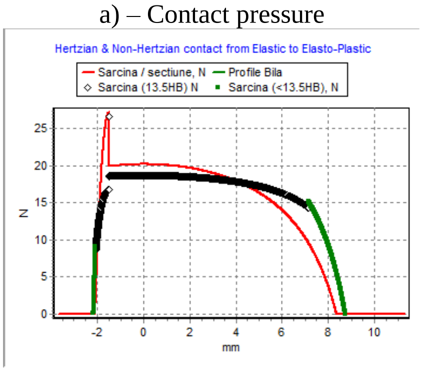


c) – Load on slices

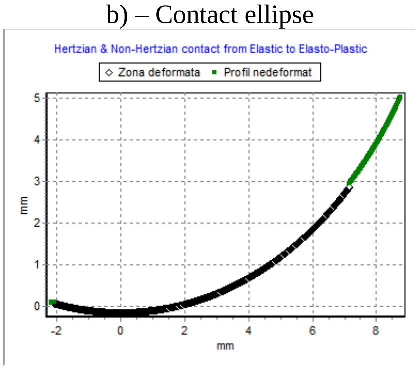


d) Indentation zones

Fig. 6.3.

## 3. CONCLUSIONS

An new analytic- numeric technique has been developed to simulate the transition form Hertzian Contact by elasto-plastic to full plastic contact, using methodology presented in [4, 5]. The values from [6] are also obtained. That method can be also used for cutting point contact (elastic non-Hertzian contact) for roller and ball bearings.

## REFERENCES

1. Harris T. A., Rolling bearing analysis, 3rd edition, 1991.
2. Johnson K. L, Contact Mechanics, Cambridge University Press, 1985.
3. Ledrappier F., Méthodologie d'étude pour optimiser la tenue en fatigue superficielle de dépôts minces – Phd Thèse – L'école centrale de Lyon, 2005.
4. Rezmireş D., Nelias D., Racocea C., Hertzian and Non-Hertzian Contact Analysis in Ball, , the Annals of "Dunărea de Jos" University of Galați, fascicle VIII, pp. 105-108, 2004.
5. Rezmires D., Research about Dynamics and Kinematics Optimization of the Spherical Roller Bearings, Iasi, PhD Thesis, 2003.
6. Standard Test Method for Brinell Hardness of Metallic Materials, American Association State Highway and Transportation Officials Standard AASHTO No.: T70–86, E 10 – 01, June 2004.
7. Kogut L., Etsion I., Elastic-Plastic Contact Analysis of a Sphere and a Rigid Flat, Journal of Applied Mechanics, Transactions of the ASME, Vol. 69, September, pp. 657-662, 2002.
8. Kogut L., Etsion I., A Semi-Analytical Solution for the Sliding Inception of a Spherical Contact, Journal of Tribology, July 2003, Vol. 125, pp. 499-506, 2003.
9. Robert L., Green I., A Finite Element Study of Elasto-Plastic Hemispherical Contact Against a Rigid Flat, Journal of Tribology, ASME, April, Vol. 127 (2), pp. 343-354, 2005.